RSC Advances

ROYAL SOCIETY OF CHEMISTRY

www.rsc.org/advances

Cite this: DOI: 10.1039/c0xx00000x

www.rsc.org/xxxxxx

ARTICLE TYPE

Enhanced mechanical properties of ammonia modified graphene nanosheets/epoxy nanocomposites

Dong-Dong Zhang, Dong-Lin Zhao,* Ran-Ran Yao and Wei-Gang Xie

Received (in XXX, XXX) Xth XXXXXXXXX 20XX, Accepted Xth XXXXXXXXX 20XX

DOI: 10.1039/b000000x

Ammonia modified graphene nanosheets (AMGNSs)/epoxy nanocomposites were prepared by using a facile blend method. Graphene nanosheets (GNSs) were modified with aqueous ammonia (NH_3•H_2O) and hydrogen peroxide (H_2O_2), to obtain amine ($–NH_2$) functionalized GNSs and enhance the bondings between the GNSs and epoxy resin matrix. The effects of AMGNSs on the static and dynamic mechanical properties of the nanocomposites were investigated. The results indicated that the tensile and flexural strength and modulus of the AMGNSs/epoxy nanocomposites increased firstly and then decreased with the increasing of AMGNS addition. The addition of 0.5 wt.% AMGNSs improved the tensile strength and flexural modulus of the pristine epoxy by 27.84% and 7.75%, respectively. Meanwhile, the addition of 0.1 wt.% AMGNSs improved the tensile modulus and flexural strength of the pristine epoxy by 14.16% and 94.38%, respectively. The reinforcing effect of AMGNSs in enhancing the impact properties of epoxy nanocomposites was also be examined. It was demonstrated that the amine functionalized GNSs by ammonia had an obvious effect on the mechanical performances of epoxy matrix nanocomposites.

1. Introduction

Graphene, a single-layer carbon sheet of sp^2-hybridized carbon atoms arranged in a hexagonal packed lattice structure, has shown many remarkable properties, such as excellent electronic transport properties, high specific surface area, high thermal conductivity and extraordinary mechanical properties.[1-8] In fact, carbon-based fillers (carbon black, carbon nanotubes, etc.) have been extensively researched as reinforcements of polymer nanocomposites for the past decades.[9] Carbon nanotubes, as the strongest contender of graphene in the nanocomposites field, are not ideal for toughening or reinforcing polymer composites, because of high viscosity, prohibitively high cost, and high anisotropic functionality.[9,10] As a new allotrope of elemental carbon, graphene has been used as a new carbon-based filler for polymer nanocomposites to obtain remarkable physical and mechanical properties.[11-17]

Epoxy resin systems are important thermoset materials used as adhesives, coatings, structural materials, insulating materials, and many other industrial applications at present.[9] Graphene-reinforced epoxy resin nanocomposites have been investigated in view of their enhanced mechanical and thermal properties.[6,9,18-26] However, the bad dispersion homogeneousness due to the high specific surface area of graphene and the weak interfacial interactions between graphene and epoxy resin, which restricts the application of graphene in polymer nanocomposites.[27-29] It is likely that the proper chemical modification of graphene can prevent the aggregation of graphene sheets as well as improve the interfacial interactions between graphene and epoxy resin and processability.[16,30,31]

In this study, we focused on the homogeneous dispersion of graphene and the changes of mechanical properties with its content increasing. As previously studied for carbon-based fillers, dispersion and interfacial interactions are two main issues governing the properties of nanocomposites.[20] Graphene obtained from reduction of graphene oxide contains carboxylic functional groups at their edges, which could provide the active sites to react with aqueous ammonia. And the amine ($–NH_2$) functionalization of graphene nanosheets (GNSs) could obviously enhance the interfacial adhesion between GNSs and the epoxy resin.[19,32] Herein, the GNSs were surface-treated with aqueous ammonia (NH_3•H_2O) and hydrogen peroxide (H_2O_2, 30%), to obtain amine functionalized GNSs and enhance the bonding between the GNSs and epoxy resin matrix. Meanwhile, the effects of ammonia modified GNSs (AMGNSs) on the static and dynamic mechanical properties and the freeze-fractured morphologies of AMGNSs/epoxy nanocomposites were investigated.

2. Experimental

2.1 Materials

Natural flake graphite (320 mesh) was purchased from Dongxin Electrical Carbon Co. Ltd., China. Concentrated sulfuric acid (H_2SO_4, 95-98%), potassium permanganate ($KMnO_4$) and concentrated hydrochloric acid (HCl, 36-38%) were all obtained from Beijing Yili Fine Chemical Co. Ltd. Hydrogen peroxide (H_2O_2, 30%), ammonia water (NH_3·H_2O) and sodium nitrate ($NaNO_3$) were obtained from Beijing Chemical Works. Epoxy resin (E-51, WSR618) based on bisphenol-A with an epoxy value of 0.50-0.56 was obtained from Wuxi Resin Factory, China. The

anhydride hardener (methyl tetrahydrophthalic anhydride, MeTHPA) and the accelerator (2,4,6-Tris (dimethylaminomethyl)phenol, DMP-30) were obtained from Beijing Chem. Reagent Co., China.

2.2 Preparation of GNSs

The modified Hummers method was conducted to oxidize natural flake graphite (320 meshes) for the synthesis of graphite oxide.[33] Typically, 3.0 g of flake graphite, 1.5 g of $NaNO_3$ and 69 ml of H_2SO_4 (95-98%) were mixed in an ice bath and then were stirred for 15 min utilizing a magnetic stirring apparatus. Subsequently, 9.0 g of $KMnO_4$ was gradually added. The mixture was allowed to react at 35 ^oC for 60 min. Then, 138 ml of distilled water (DI water) was gradually added into the mixture within 10 min and then the mixture was allowed to react at 98 ^oC for 15 min. Then the solution was terminated by adding 420 ml of DI water and 30 ml of 30% H_2O_2 solution, resulting in a yellow-brown mixture. Then the mixture was centrifuged at 4000 rpm for 5 min and washed at least three times with a solution of 5% HCl until sulphate could not be detected with $BaCl_2$. The obtained graphite oxide deposits were dispersed in 500 ml of DI water utilizing a high-power ultrasonic machine for 1.5 h. Then the solution was centrifuged again at 4000 rpm for 5 min to eliminate insoluble substance. After centrifugation, 150 ml of HCl (36-38%) was added into the supernatant liquid and then the suspension was centrifuged again at the same conditions. After graphite oxide was dried at 65 ^oC in the air for 24 h, it was placed into a ceramic crucible to be heated at 1050 ^oC for 30 s in muffle furnace. Consequently, the resulting expanded graphite was dispersed in ethanol as a ratio of 0.2g/100ml. And then the suspension was sonicated for 15 h utilizing a high-power ultrasonic machine. Finally, after removing the redundant ethanol in the suspension, the mixture was heated at 120 ^oC for 4 h in a vacuum oven to get GNSs.

2.3 Preparation of AMGNSs

Briefly, 1.5 g GNSs firstly was added into 240 ml mixed solution of H_2O_2 (30%) and $NH_3 \cdot H_2O$ at a volume ratio of 3:5. Then, the mixture was stirred at room temperature for 15 min. Consequently, the solution was treated under sonication for 4 h. After that, the resultant alkali-treated GNSs were filtrated using a core funnel and washed at least three times with DI water until the solution was neutral. After flltration, the mixture was dried at 65 ^oC for 12 h in a vacuum oven to get AMGNSs.

2.4 Preparation of AMGNSs/epoxy nanocomposites

The weight ratio of epoxy to MeTHPA, 1:0.7, was used to prepare the AMGNSs/epoxy nanocomposites. Afterwards, the AMGNSs was manually mixed with a mixture of epoxy and MeTHPA. Then, the suspension was treated under sonication for 3 h to make AMGNSs homogeneous dispersion in the epoxy system. After few drops of DMP-30 (accelerator) were added into the mixture, more 30 min ultrasonication was needed. The resultant suspension was degassed with a vacuum oven at 50 ^oC for 30 min to remove air bubbles. Consequently, the mixture was poured into stainless steel mold to cure at 90 ^oC for 1 h, 130 ^oC for 2 h, and then 160 ^oC for 2 h. After curing, the nanocomposite samples were cooled naturally to room temperature. The AMGNS weight fractions of 0 wt.%, 0.05 wt.%, 0.1 wt.%, 0.5 wt.%, and 1 wt.% were prepared.

2.5 Characterization techniques and instruments

The morphologies of GNSs and AMGNSs were investigated by transmission electron microscope (TEM, Hitachi H-800). Fourier transform infrared spectroscopy (FT-IR) spectra of GNSs and AMGNSs were recorded on a Nicolet Nexus 670 FT-IR spectrometer. Tensile and flexural tests were carried out with an Instron^{TM} 1185 mechanical testing machine at room temperature with crosshead speed of 10 mm/min and 5 mm/min, respectively. The tensile specimens were standard dumbbell-shaped according to GB/T 1040-1992 (Fig. 1), and the geometric dimensions of the samples for flexural tests were 80 mm (length)×15 mm (width)×4 mm (thickness) according to GB/T 9341-2008 (Fig. 2). The freeze-fractured surfaces of AMGNSs/epoxy nanocomposites with different AMGNSs contents were observed by scanning electron microscope (SEM, S-4700). The dynamic mechanical properties of AMGNSs/epoxy nanocomposites were performed on a dynamic mechanical analysis (DMA) VA3000 (01dB-Metravib Instruments Inc., France) at the frequency of 1 Hz from 25 to 200 ^oC at the heating rate of 5 ^oC/min. The geometric dimensions of DMA samples were 50 mm (length)×6 mm (width)×2 mm (thickness). The Charpy impact strength of the samples was tested with a Resil Impactor 6957 (Ceast Instruments Inc., Italy) according to GB/T 2571-1995.

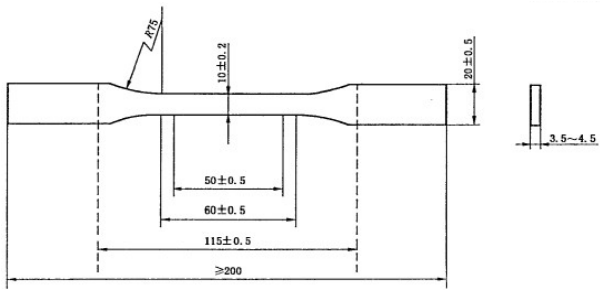

Fig. 1 Tensile test sample geometry (unit: mm).

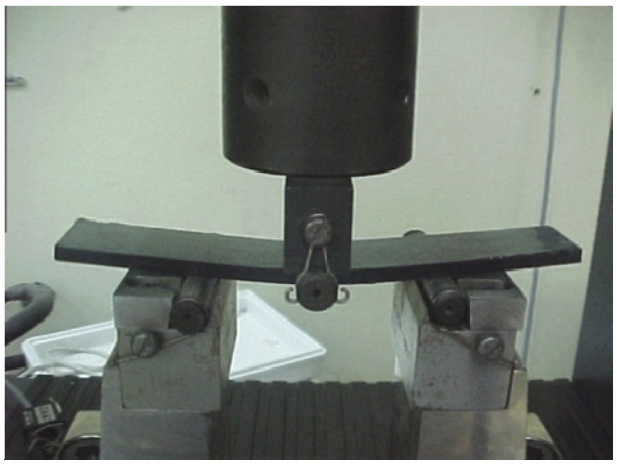

Fig. 2 Three-point bending mode for flexural tests.

3. Results and discussions

3.1 Characterization of GNSs and AMGNSs

The morphology and structure of GNSs and AMGNSs were characterized by TEM. As shown in Fig. 3, GNSs and AMGNSs

are consisted of almost transparent carbon nanosheets with thin wrinkled structure. Both GNSs and AMGNSs are entangled with each other and resemble crumpled papers. Meanwhile, the curled and corrugated structure is the intrinsic characteristic of graphene. It is well known that as-prepared GNSs still contains carboxylic functional groups at their edges, which could provide the active sites to react with aqueous ammonia, as illustrated in Fig. 4a.[19,32,34] The covalent modification of graphene can be achieved in four different ways: nucleophilic substitution, electrophilic addition, condensation, and addition. The main reactive sites in the nucleophilic substitution reaction are the epoxy groups of graphene oxide or graphene. The amine ($–NH_2$) functionality of the modifiers bearing a lone pair of electrons attacks the epoxy groups of the graphene oxide or graphene. In comparison to other methods, nucleophilic substitution occurs very easily, also at room temperature and in an aqueous medium. Therefore, this method has been considered to be a promising method for large-scale production of functionalized graphene.[16] In general, ammonia can interact with carboxylic functional groups at the edges of the GNSs as either Brønsted acids into $NH4^+$ or Lewis acids into $–NH_2$,[32] as illustrated in Fig. 4b and c, which was further supported by FT-IR spectra of AMGNSs in Fig. 5. By ammonia-treatment, the AMGNSs have absorption peaks at wave numbers of 3430 cm^{-1} (the O-H stretching vibration of terminal carboxyl groups), 1560 cm^{-1} (the N-H bending vibration of primary amide), 1400 cm^{-1} (the C-N stretching vibration of primary amide), and 727 cm^{-1} (the C-N stretching vibration of amine), respectively. It indicates that mixed ammonia solution successfully modified the surfaces of GNSs, resulting an improvement of the interfacial interactions between AMGNSs and epoxy resin. And all of the characteristic peaks behave blue-shifting (shift to low wavenumbers) after ammonia modification ascribing to the amine ($–NH_2$) functionalization of the GNS.

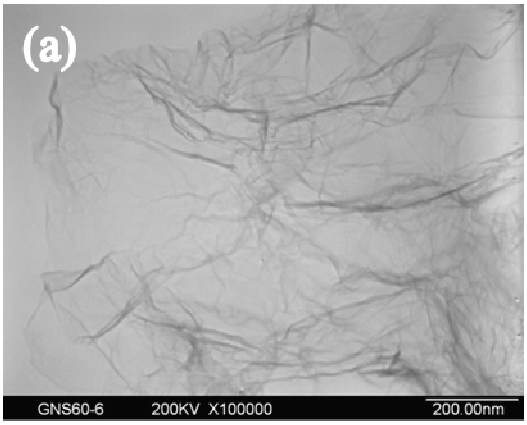

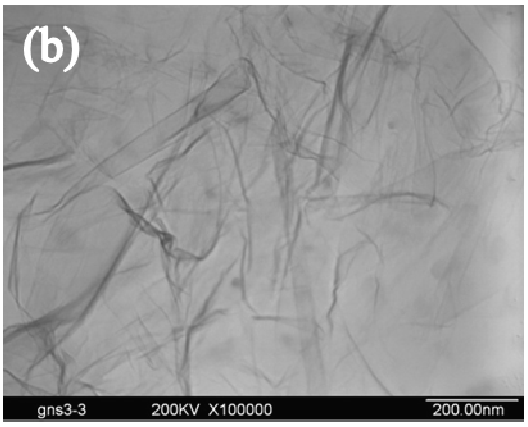

Fig. 3 TEM images of GNSs (a) and AMGNSs (b).

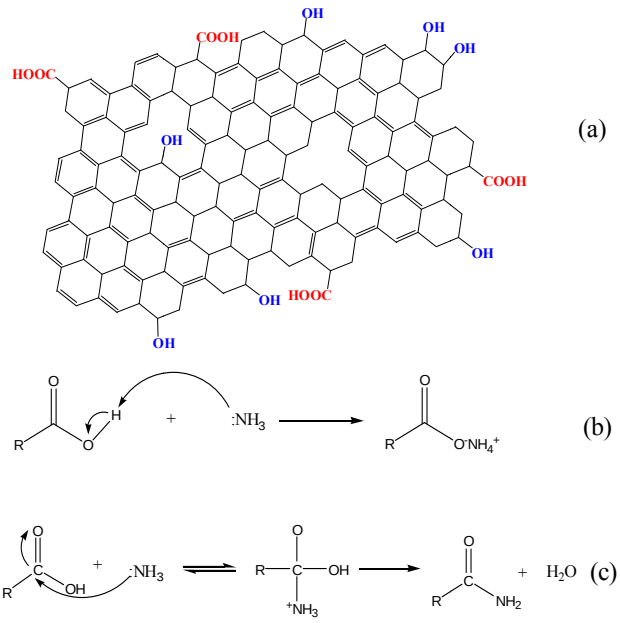

Fig. 4 Scheme of structure model of GNS (a), and proposed reaction mechanism for oxygen-containing functional groups and ammonia: (b) ammonia interacts with carboxylic groups as Brønsted acid into NH_4^+; (c) carboxylic groups interact with ammonia as Lewis acids into $–NH_2$

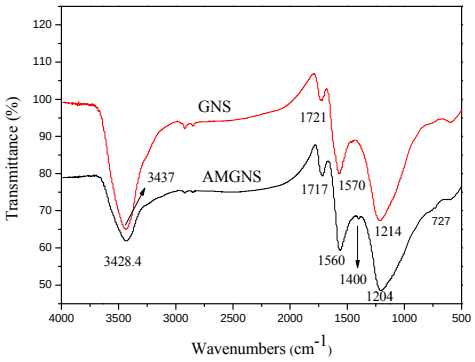

Fig. 5 FT-IR spectra of GNSs and AMGNSs.

3.2 Morphological analysis of AMGNSs/epoxy nanocomposites

In order to evaluate the interfacial interactions between AMGNSs

and epoxy matrix and the dispersion of AMGNSs in the samples, the freeze-fractured surfaces of AMGNSs/epoxy nanocomposites were further investigated by SEM. Fig. 6 shows that the pristine epoxy has smooth and featureless fracture surface (Fig. 6a), and the freeze-fractured surface of the 0.1 wt.% AMGNSs-filled epoxy nanocomposites shows some cracks and AMGNSs can be observed to be pulled out (Fig. 6b). Then, as the further increase of AMGNS content, most AMGNSs disperse well and have a good crosslinking state in the epoxy resin (Fig. 6c and d). Moreover, a linear stripe morphology of the AMGNSs in epoxy resin is also observed in Fig. 6c and d. The fracture surface of neat epoxy is comparatively smooth, indicating a lower ductility. By adding AMGNSs into the epoxy resin, the toughness increased with AMGNS content, making the fracture surface much rougher. These results indicate that the AMGNSs may inhibit the propagation of cracks and thus increase the strain energy required for fracture.

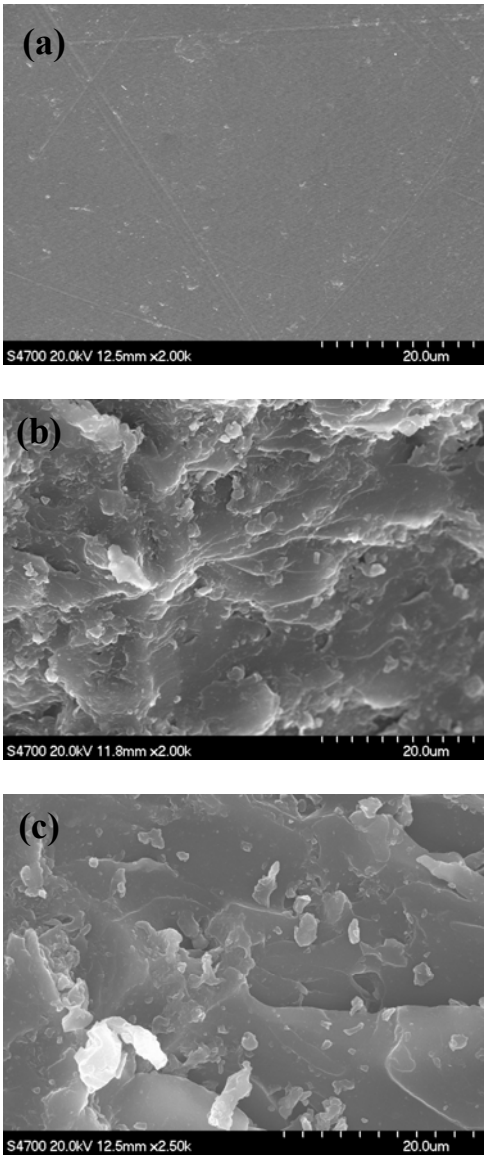

Fig. 6 SEM images of the freeze-fractured surfaces of AMGNSs/epoxy nanocomposites for AMGNS contents of (a) 0 wt.%, (b) 0.1 wt.%, (c) and (d) 0.5 wt.%.

3.3 Tensile properties of AMGNSs/epoxy nanocomposites

The effect of AMGNS content on the tensile properties of AMGNSs/epoxy nanocomposites are shown in Fig. 7. From Fig. 7a and b, both the tensile strength and elongation at break of AMGNSs/Epoxy nanocomposites increase steadily with increasing the weight fractions of AMGNSs up to 0.5 wt.% and dropped slightly at 1 wt.%. The 0.5 wt.% AMGNSs-filled epoxy matrix increases the tensile strength and elongation at break of pristine epoxy to 67.28 MPa and 4.29%, 27.84% and 63.74% increments, respectively. From Fig. 7c, it can be seen that the most significant improvement of the tensile modulus was obtained at 0.1 wt.% AMGNSs reaching 2.81 GPa which was an increase of 14.16% compared to pristine epoxy.

Representative tensile stress versus strain curves are shown in Fig. 8. It can be seen that, both the tensile strength and the area under the stress-strain curve reach the maximum value at AMGNS loading of 0.5 wt.%. Combining Figs. 7 and 8, we can conclude that the proper surface-modification of AMGNSs can result in a significant increase in tensile properties due to the homogeneous dispersion for AMGNSs in epoxy resin and the strong interfacial interactions between filler and epoxy resin, resulting in effective load transfer from epoxy resin to AMGNS filler. However, the lower strength at higher AMGNS concentration (≥1.0 wt.%) can be attributed to the inevitable aggregation of AMGNSs at high concentration.[18,35]

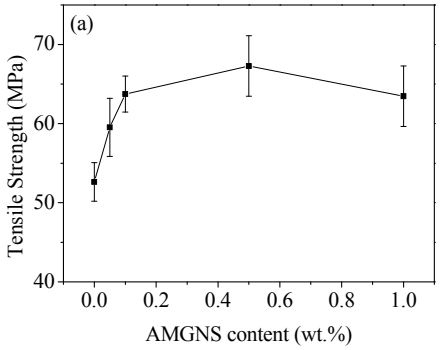

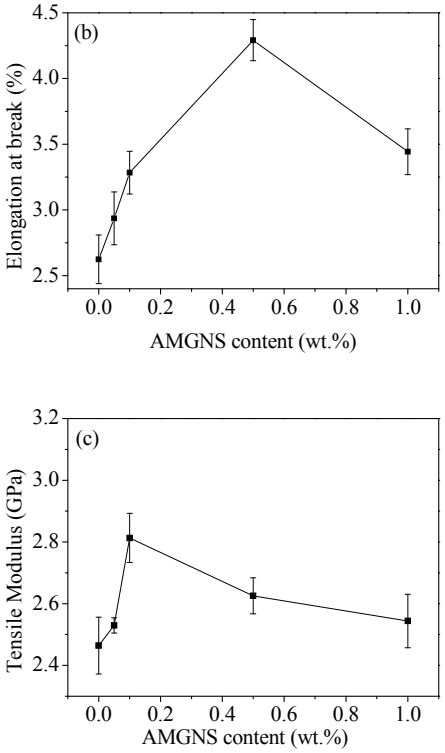

Fig. 7 The effects of AMGNS loading content (wt.%) on the tensile properties of AMGNSs/epoxy nanocomposites: tensile strength (a), elongation at break (b) and tensile modulus (c).

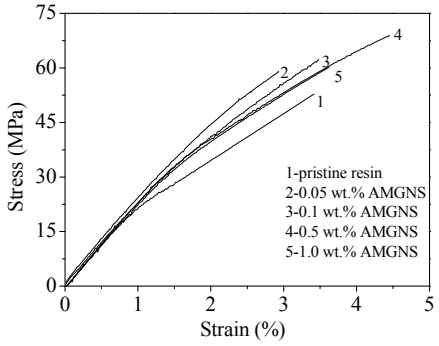

Fig. 8 Stress-strain curves for AMGNSs/epoxy nanocomposites under tensile loading.

3.4 Flexural properties of AMGNSs/epoxy nanocomposites

Fig. 9 shows the results of three-point bending test of AMGNSs/epoxy nanocomposites. It is found that all samples filled with AMGNSs show significant improvement in flexural properties compared to pristine epoxy. As can be seen, the 0.1 wt.% AMGNSs-filled epoxy nanocomposites shows the maximum flexural strength as high as 135.58 MPa, which is an increase of 94.38% compared to pristine epoxy and almost an increase of 37.32% compared to 0.5 wt.% AMGNSs-filled epoxy nanocomposites. Meanwhile, the 0.5 wt.% AMGNSs-filled epoxy nanocomposites shows the maximum flexural modulus as high as 3.48 GPa, which is an increase of 7.75% compared to pristine epoxy. Then, it is found that when the loading of AMGNSs reaches 1.0 wt.% the flexural properties of AMGNSs/epoxy nanocomposites begin to descend due to the agglomeration of AMGNSs at high content. Above studies agree with the previous work that addition of graphene nanoplatelet result in an increase of mechanical properties for nanocomposites even at small amount of filler.[18]

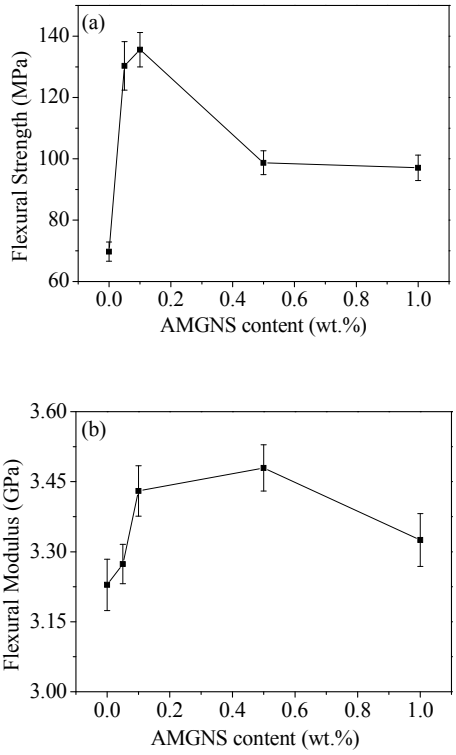

Fig. 9 The effects of AMGNS loading content (wt.%) on the flexural properties of AMGNSs/epoxy nanocomposites: flexural strength (a) and flexural modulus (b).

3.5 Impact strength of AMGNSs/epoxy nanocomposites

The impact strength of AMGNSs/epoxy nanocomposites are shown in Fig. 10. From Fig. 10, the impact strength of AMGNSs/epoxy nanocomposites improves with increasing the weight fractions of AMGNSs in epoxy matrix and increases by 34.3% from 15.65 to 21.02 MPa at AMGNS loading of 0.1 wt.%. The remarkable influence on the impact strength of nanocomposites at low AMGNS loading can be attributed to a good dispersion and a strong interfacial interaction, which can effectively hinder the formation and propagation of cracks in the samples.[36,37] As a result, the surfaces of the nanocomposites shown in Fig. 6b are rougher than those of the pure epoxy matrix shown in Fig. 6a. Then, the impact strength of AMGNSs/epoxy nanocomposites gradually decreases with further increasing the AMGNS content due to the weak dispersion and bad processability of the nanocomposites. Since the negative deteriorating effect of the AMGNS aggregation would overwhelm the toughening effect of the AMGNSs indicated by the rough fracture surfaces for the high AMGNS contents of 0.5 wt.% (Fig. 6d). Thus, a decrease in the composite impact strength is observed by the addition of the graphene at a relatively high content.

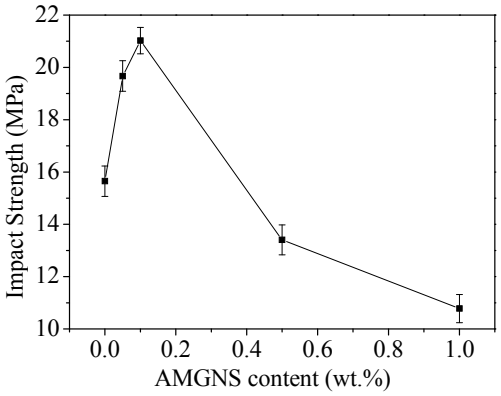

Fig. 10 The effects of AMGNS loading content (wt.%) on the impact strength of AMGNSs/epoxy nanocomposites.

3.6 DMA of AMGNSs/epoxy nanocomposites

DMA provides information on storage modulus and loss angle tangent curves of AMGNSs/epoxy nanocomposites as a function of temperature.[9] As shown in Fig. 11a, the storage modulus of AMGNSs/epoxy nanocomposites improve continuously with increasing the AMGNS content in epoxy matrix. The storage modulus have obviously increased from 0.83 GPa for pristine epoxy to 1.31 GPa for 1.0 wt.% AMGNSs-filled epoxy nanocomposites at the initial temperature (50 ^{o}C), which is a 57.83% increase. The storage modulus of all samples fall with temperature due to the transition of the glassy plateau to the rubbery plateau. The Tg values were taken as the maximum of the tan δ curves. As shown in Fig. 11b, the glass transition temperature (Tg) began at about 133 ^{o}C for pristine epoxy. The Tg of AMGNSs/epoxy nanocomposites containing low content of AMGNSs (≤0.5 wt.%) shift to higher temperatures of about 137-141 ^{o}C and have a narrower temperature range due to the strong interfacial interaction between AMGNSs and epoxy matrix. From Fig. 11a and b, the mechanical improvement could be attributed to the high specific surface area of AMGNSs with the wrinkled structure and the enhanced interfacial interaction of filler-matrix.[38]

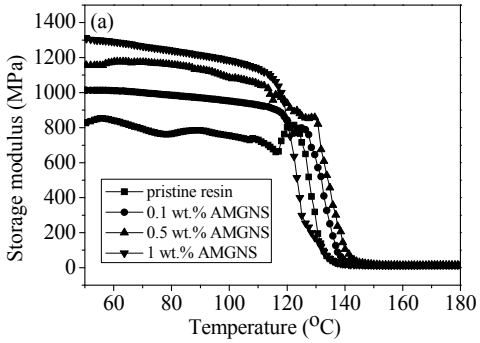

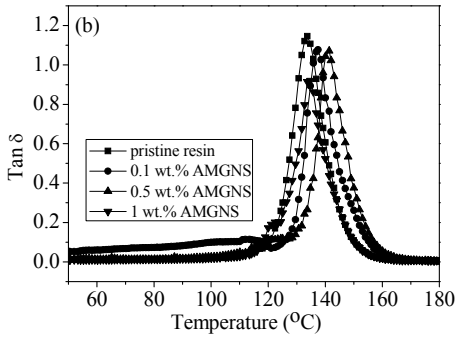

Fig. 11 The effects of AMGNS loading content (wt.%) on DMA of the AMGNSs/epoxy nanocomposites: (a) Storage modulus spectra and (b) Tan δ spectra.

4. Conclusions

GNSs were amine functionalized by NH_3•H_2O and H_2O_2 to achieve better affinity to the epoxy matrix. The presence of the functional groups was verified by FT-IR spectroscopy. The effective modification of GNSs with ammonia was confirmed to improve the interfacial interaction between AMGNSs and epoxy resin, resulting in an increase of mechanical properties. Thus, AMGNSs could play a reinforcement role in the epoxy matrix.

The mechanical results showed that the addition of AMGNSs at 0.1 wt.% loading into the pristine epoxy could reach the most significant improvements of tensile modulus (+14.16%), flexural strength (+94.38%) and impact strength (34.3%). Moreover, the most significant improvements of tensile strength (+27.84%) and flexural modulus (+7.75%) were attained with AMGNSs at a 0.5 wt.% content. The glass transition temperature (Tg) of pristine epoxy was increased from 133 to 137 ^{o}C at 0.1 wt.% AMGNSs and 141 ^{o}C at 0.5wt.% AMGNSs, respectively.

Acknowledgements

This work was supported by the National Natural Science Foundation of China (Grant No. 50672004), National High-Tech Research and Development Program (2008AA03Z513) and Doctoral Fund of Ministry of Education of China (20120010110001).

Notes and references

State Key Laboratory of Chemical Resource Engineering; Key Laboratory of Carbon Fiber and Functional Polymers (Beijing University of Chemical Technology)，Ministry of Education; Beijing Engineering Research Center of Environmental Material for Water Purification; Beijing University of Chemical Technology, Beijing 100029, China.

**Corresponding author: Fax: +86 10 64434914; Tel: +86 10 64434914; E-mail: dlzhao@mail.buct.edu.cn (Prof. Dong-Lin Zhao)*

† Electronic Supplementary Information (ESI) available: [details of any supplementary information available should be included here]. See DOI: 10.1039/b000000x/

‡ Footnotes should appear here. These might include comments relevant to but not central to the matter under discussion, limited experimental and spectral data, and crystallographic data.

1 K. S. Novoselov, A. K. Geim, S. V. Morozov, D. Jiang, Y. Zhang, S. V. Dubonos, I. V. Grigorieva and A. A. Firsow, *Science*, 2004, **306**, 666-669.

2 A. K. Geim and K. S. Novoselov, *Nat. Mater.*, 2007, **6**, 183-191.

3 G. Wang, J. Yang, J. Park, X. Gou, B. Wang, H. Liu and J. Yao, *Phys. Chem. C*, 2008, **112**, 8192-8195.
4 G. Wang, X. Shen, J. Yao and J. Park, *Carbon*, 2009, **47**, 2049-2053.
5 X. Li, X. Wang, L. Zhang, S. Lee and H. Dai, *Science*, 2008, **319**, 1229-1231.
6 M. Martin-Gallegoa, R. Verdejoa. M. A. Lopez-Manchadoa and M. Sangermano, *Polymer*, 2011, **52**, 4664-4669.
7 C. Lee, X. Wei, J. W. Kysar and J. Hone, *Science*, 2008, **321**, 385-388.
8 A. A. Balandin, S. Ghosh, W. Bao, I. Calizo, D. Teweldebrhan, F. Miao and C. N. Lau, *Nano Lett.*, 2008, **8**, 902-907.
9 I. Zaman, T. T. Phan, H. C. Kuan, Q. Meng, L. T. Bao La, L. Luong, O. Youssf and J. Ma, *Polymer*, 2011, **5**, 1603-1611.
10 N. Roy, R. Sengupta and A. K. Bhowmick, *Prog. Polym. Sci.*, 2012, **37**, 781-819.
11 C. Bao, Y. Guo, L. Song, Y. Kan, X. Qian and Y. Hu, *J. Mater. Chem.*, 2011, **21**, 13290-13298.
12 H. Kim, Y. Miura and C. W. Macosko, *Chem. Mater.*, 2010, **22**, 3441-3450.
13 Y. Shao, J. Wang, H. Wu, J. Liu, I. A. Aksay and Y. Lin, *Electroanalysis*, 2010, **22**, 1027-1036.
14 X. Huang, X. Qi, F. Boey and H. Zhang, *Chem. Soc. Rev.*, 2012, **41**, 666-686.
15 J. R. Potts, D. R. Dreyer, C. W. Bielawski and R. S. Ruoff, *Polymer*, 2011, **52**, 5-25.
16 T. Kuila, S. Bose, A. K. Mishra, P. Khanra, N. H. Kim and J. H. Lee, *Prog. Mater. Sci.* 2012, **57**, 1061-1105.
17 R. Sengupta, M. Bhattacharya, S. Bandyopadhyay and A. K. Bhowmick, *Prog. Polym. Sci.*, 2011, **36**, 638-670.
18 M. A. Rafiee, J. Rafiee, Z. Wang, H. Song, Z. Z. Yu and N. Koratkar, *ACS Nano*, 2009, **3**, 3884-3890.
19 X. Wang, W. Xing, P. Zhang, L. Song, H. Yang and Y. Hu, *Compos. Sci. Technol.*, 2012, **72**, 737-743.
20 S. Chatterjee, J. W. Wang, W. S. Kuo, N. H. Tai, C. Salzmann, W. L. Li, R. Hollertz, F. A. Nüesch and B. T. T. Chu, *Chem. Phys. Lett.*, 2012, **531**, 6-10.
21 S. Zhao, L. S. Schadler, R. Duncan, H. Hillborg and T. Auletta, *Compos. Sci. Technol.*, 2008, **68**, 2965-2975.
22 B. B. Johnsen, A. J. Kinloch, R. D. Mohammed, A. C. Taylor and S. Sprenger, *Polymer*, 2007, **48**, 530-541.
23 A. Yasmin and I. M. Daniel, *Polymer*, 2004, **45**, 8211-8219.
24 P. Guo, X. Chen, X. Gao, H. Song and H. Shen, *Compos. Sci. Technol.*, 2007, **67**, 3331-3337.
25 J. N. Coleman, U. Khan and Y. K. Gun'ko, *Adv. Mater.*, 2006, **18**, 689-706.
26 H. Yang, C. Shan, F. Li, Q. Zhang, D. Han and L. Niu, *J. Mater. Chem.*, 2009, **19**, 8856-8860.
27 T. Ramanathan, A. A. Abdala, S. Stankovich, D. A. Dikin, M. Herrera-Alonso, R. D. Piner, D. H. Adamson, H. C. Schniepp, X. Chen, R. S. Ruoff, S. T. Nguyen, I. A. Aksay, R. K. Prud'Homme and L. C. Brinson, *Nat. Nanotechnol.*, 2008, **3**, 327-331.
28 J. Zhu, *Nat. Nanotechnol.*, 2008, **3**, 528-529.
29 T. Kuilla, S. Bhadra, D. Yao, N. H. Kim, S. Bose and J. H. Lee, *Prog. Polym. Sci.*, 2010, **35**, 1350-1375.
30 K. A. Worsley, P. Ramesh, S. K. Mandal, S. Niyogi, M. E. Itkis and R. C. Haddon, *Chem. Phys. Lett.*, 2007, **445**, 51-56.
31 S. Niyogi, E. Bekyarova, M. E. Itkis, J. L. McWilliams, M. A. Hamon and R. C. Haddon, *J. Am. Chem. Soc.*, 2006, **128**, 7720-7721.
32 M. Seredych and T. J. Bandosz, *J. Phys. Chem. C*, 2007, **111**, 15596-15604.
33 W. S. Hummers and R. E. Offeman, *J. Am. Chem. Soc.*, 1958, **80**, 1339.
34 P. Guo, H. Song and X. Chen, *J. Mater. Chem.*, 2010, **20**, 4867-4874.
35 X. J. Shen, Y. Liu, H. M. Xiao, Q. P. Feng, Z. Z. Yu and S. Y. Fu, *Compos. Sci. Technol.*, 2012, **72**, 1581-1587.
36 J. P. Yang, G. Yang, G. Xu and S. Y. Fu, *Compos. Sci. Technol.*, 2007, **67**, 2934-2940.
37 L. Wang, K. Wang, L. Chen, Y. Zhang and C. He, *Composite Part A*, 2006, **37**, 1890-1896.
38 M. A. Rafiee, J. Rafiee, Z. Z. Yu and N. Koratkar, *Appl. Phys. Lett.*, 2009, **95**, 223103-223103-3.